Prediction of Response to Temozolomide in Low-Grade Glioma Patients Based on Tumor Size Dynamics and Genetic Characteristics

P Mazzocco, Célia Barthélémy, G Kaloshi, Marc Lavielle, D Ricard, A Idbaih,
D Psimaras, M-A Renard, A Alentorn, J Honnorat, et al.

HAL Id: hal-01252076

https://hal.archives-ouvertes.fr/hal-01252076

Submitted on 7 Jan 2016

ORIGINAL ARTICLE

Prediction of Response to Temozolomide in Low-Grade Glioma Patients Based on Tumor Size Dynamics and Genetic Characteristics

P Mazzocco[1], C Barthélémy[2], G Kaloshi[3], M Lavielle[2], D Ricard[4], A Idbaih[3], D Psimaras[3], M-A Renard[3], A Alentorn[3], J Honnorat[5], J-Y Delattre[3], F Ducray[5] and B Ribba[1]*

Both molecular profiling of tumors and longitudinal tumor size data modeling are relevant strategies to predict cancer patients' response to treatment. Herein we propose a model of tumor growth inhibition integrating a tumor's genetic characteristics (p53 mutation and 1p/19q codeletion) that successfully describes the time course of tumor size in patients with low-grade gliomas treated with first-line temozolomide chemotherapy. The model captures potential tumor progression under chemotherapy by accounting for the emergence of tissue resistance to treatment following prolonged exposure to temozolomide. Using information on individual tumors' genetic characteristics, in addition to early tumor size measurements, the model was able to predict the duration and magnitude of response, especially in those patients in whom repeated assessment of tumor response was obtained during the first 3 months of treatment. Combining longitudinal tumor size quantitative modeling with a tumor''s genetic characterization appears as a promising strategy to personalize treatments in patients with low-grade gliomas.

Study Highlights

WHAT IS THE CURRENT KNOWLEDGE ON THE TOPIC? ☑ First-line temozolomide is frequently used to treat low-grade gliomas (LGG), which are slow-growing brain tumors. The duration of response depends on genetic characteristics such as 1p/19q chromosomal codeletion, p53 mutation, and IDH mutations. However, up to now there are no means of predicting, at the individual level, the duration of the response to TMZ and its potential benefit for a given patient. • WHAT QUESTION DID THIS STUDY ADDRESS? ☑ The present study assessed whether combining longitudinal tumor size quantitative modeling with a tumor's genetic characterization could be an effective means of predicting the response to temozolomide at the individual level in LGG patients. • WHAT THIS STUDY ADDS TO OUR KNOWLEDGE ☑ For the first time, we developed a model of tumor growth inhibition integrating a tumor's genetic characteristics which successfully describes the time course of tumor size and captures potential tumor progression under chemotherapy in LGG patients treated with first-line temozolomide. The present study shows that using information on individual tumors' genetic characteristics, in addition to early tumor size measurements, it is possible to predict the duration and magnitude of response to temozolomide. • HOW THIS MIGHT CHANGE CLINICAL PHARMACOLOGY AND THERAPEUTICS ☑ Our model constitutes a rational tool to identify patients most likely to benefit from temozolomide and to optimize in these patients the duration of temozolomide therapy in order to ensure the longest duration of response to treatment.

Response evaluation criteria such as RECIST—or RANO for brain tumors—are commonly used to assess response to anticancer treatments in clinical trials.[1,2] They assign a patient's response to one of four categories, ranging from "complete response" to "disease progression." Yet, criticisms have been raised regarding the use of such categorical criteria in the drug development process,[3,4] and regulatory agencies have promoted the additional analysis of longitudinal tumor size measurements through the use of quantitative modeling.[5] Several mathematical models of tumor growth and response to treatment have been developed for this purpose.[6,7] These analyses have led to the identification of a variety of tumor size metrics that can be used to predict long-term clinical outcomes such as overall survival.[8] For instance, tumor size change 2 months after the beginning of treatment has been identified as a predictor of overall survival in non-small cell lung cancer[5] and in colorectal cancer.[9] This suggests that long-term clinical outcomes can be predicted on the basis of early tumor size dynamics.

Low-grade glioma (LGG) is a slow-growing brain tumor whose management involves the use of repeated magnetic resonance imaging (MRI) scans to monitor the size of tumor lesions. Surgery, radiotherapy, and two chemotherapy

[1]Inria, project-team Numed, Ecole Normale Supérieure de Lyon, Lyon, France; [2]Inria, project-team Popix, Université Paris-Sud, Orsay, France; [3]AP-HP, Groupe Hospitalier Pitié-Salpêtrière, Service de Neurologie Mazarin; INSERM, U975, Centre de Recherche de l'Institut du Cerveau et de la Moelle, Université Pierre & Marie Curie Paris VI, Faculté de Médecine Pitié-Salpêtrière, CNRS UMR 7225 and UMR-S975, Paris, France; [4]Hôpital d'instruction des Armées du Val-de-Grâce, Paris, France; [5]Hospices Civils de Lyon, Hôpital Neurologique, Neuro-oncologie; Université de Lyon, Claude Bernard Lyon 1, Lyon Neuroscience Research Center INSERM U1028/CNRS UMR, Lyon, France. *Correspondence: B Ribba (benjamin.ribba@inria.fr)

Prediction of Low-Grade Glioma Response to TMZ
Mazzocco *et al*.

729

regimens, PCV (procarbazine, CCNU, and vincristine) and temozolomide (TMZ), constitute the standard of care.[10] Both prognosis and response to treatment—in particular to TMZ therapy—have been shown to depend on genetic or molecular characteristics such as 1p/19q chromosomal codeletion,[11,12] p53 mutation,[12] and IDH mutations.[13] TMZ is an orally administered molecule with proven efficacy in the first-line treatment of LGG.[14] It is generally given for 1 to 2 years, one cycle per month. The duration of the treatment is frequently prolonged beyond 12 cycles if an ongoing decrease in tumor size is observed at this time.[15] However, until now there is no way of predicting, at the individual level, the duration of the response to TMZ and its potential benefit for a given patient.

We previously proposed a tumor growth inhibition model to analyze the time-course of mean tumor diameter in LGG patients receiving chemotherapy or radiotherapy.[16] Herein, we further develop this model to analyze the time-course of tumor size in patients treated with TMZ, to characterize potential emergence of resistance to TMZ, and to identify the impact of a patient's molecular characteristics on tumor size kinetic parameters. Finally, we show that the modeling framework can leverage tumor size data obtained during the early stages of treatment, i.e., during the first few months, to forecast tumor response.

METHODS
Patients and observations
We analyzed data from 120 LGG patients treated between 1999 and 2007.[12] Data included information on tumor size in all patients and on up to three molecular (genetic) characteristics in 77 patients: 1p/19q chromosomal codeletion, p53 overexpression (a surrogate marker for TP53 missense mutations[17]), and IDH mutation status. The model was built using the data from these 77 patients. Among these patients, information on all molecular characteristics was available for 42 patients (54.5%), and information on at least one item of molecular characteristic in 35 patients (45.5%). The data from the 43 patients without molecular information were used as an external dataset to evaluate model quality.

Tumor sizes were measured manually from printed MRI images and expressed as mean tumor diameter (MTD) in millimeters, according to the formula $MTD = (2V)^{1/3}$, where $V = \frac{D_1 \times D_2 \times D_3}{2}$ is the approximated tumor volume with D_1, D_2, and D_3 referring to the three largest perpendicular diameters. The total median duration of the posttreatment follow-up period for a single patient, which included several follow-up observations, was 21 months (5 months at minimum and 9.5 years at maximum). We analyzed a total of 952 MTD observations with, on average, 12 observations per patient (minimum 4 observations and maximum 28). Histology consisted of grade II oligodendrogliomas (56 patients, 73%), oligoastrocytomas (16 patients, 21%), and astrocytomas (5 patients, 6%). All patients received TMZ as first-line treatment. The drug was administered for 5 consecutive days (day 1 to day 5) every 28 days at a daily dose of 200 mg/m².

Mathematical model of LGG response to chemotherapy
We recently proposed a mathematical model to describe MTD dynamics in LGG patients before, during, and after chemotherapy.[16] The model, which distinguishes between disease-specific and treatment-specific parameters, relies on the hypothesis that LGG tumors are made up of both quiescent and proliferative cells, and that both cell types are sensitive to treatment.[18,19] Chemotherapy is assumed to act by damaging cells' DNA. The DNA damage leads proliferative cells to die, whereas quiescent cells with DNA damage can either repair their lesions and return to a proliferative state or die. Thus, we consider three compartments: proliferative tissue, denoted P; nondamaged quiescent tissue, denoted Q; and damaged quiescent tissue, denoted Q_p. The sum of the values attributed to the three compartments (P^*) represents the size of the lesion and is compared to the MTD observations.

To allow for MTD increase during TMZ treatment, we extended the previously proposed model[16] by taking into account the possibility that proliferative cells can repair their DNA lesions during the division process, instead of immediately dying, and thus acquire resistance to TMZ. In line with previous works,[9] we implemented acquisition of resistance by assuming that the effect of TMZ concentration on tumor tissues decreases exponentially with the amount of time since the beginning of treatment. Both proliferative and quiescent tissues were considered as having the potential to acquire resistance to TMZ.

Estimation of population parameters
The model was developed in a population context,[20] and the values of individual-level parameters were assumed to be log-normally distributed; i.e., for a parameter ψ_i corresponding to an individual patient i, $\psi_i = \psi.\exp\eta_i$ where ψ is the "typical" (population) value of the parameter, and η_i represents the contribution of the individual i. The values of η are normally distributed with mean 0. Population and individual parameter values were estimated with the SAEM (Stochastic Approximation of the Expectation Maximization) algorithm implemented in Monolix 4.2 (Lixoft) using the full MTD time-course in the 77 patients. We assumed a constant error model, with parameter value a. Model selection was carried out according to the usual criteria; in particular, models that achieved lower values of the objective function ($-2 \times \log likelihood$) were considered to provide a better fit to the data.

Integration of genetic information
The data from the 42 patients with complete molecular status (codeletion 1p/19q, p53, and IDH mutations) was used as a training dataset to obtain statistics on this genetic information. We computed the percentage of patients with a given genetic profile and derived the probability to exhibit it. So for patients with one or two missing covariates, we could compute the probability to exhibit the lacking mutation status(es), knowing the other(s) one(s). We therefore attributed genetic characteristics for patients with missing covariates. In our training dataset, in line with previous literature,[12] 1p/19q codeletion and the p53 mutation were mutually exclusive. We incorporated the molecular information into the

model and identified the effect of each status on the tumor size kinetic parameters. For a given fixed-effect parameter ζ, the model used for covariate analysis was of the following form:

$$\xi_1 = \xi_0 \times \exp\left(\beta.status_j\right) \tag{1}$$

where *status$_j$* corresponds to the value of the characteristic *j*. As we considered binary variables only, Eq. 1 could be simplified:

$$\xi_1 = \xi_0 \times \exp\left(\beta\right)$$

where ξ_0 denotes the population value of the parameter for the reference group of patients (with non-codeleted 1p/19q or wild p53), and ξ_1 is the population value for the group of patients with mutated covariate.

Using this framework, only fixed-effect parameters can depend on the covariate status while (interindividual) variability is not concerned, i.e., parameters ξ_0 and ξ_1 will have the same variability.

We used a stepwise forward/backward modeling strategy based on progressive inclusion and then exclusion of covariates, where the decision to include or exclude a covariate was dependent on the covariate's effect on the objective function through a log-likelihood ratio test.[21]

Empirical Bayes estimates to predict LGG response to temozolomide

Following a Bayesian approach in which population parameter estimates constituted prior information, we analyzed each patient's data individually, considering only the MTD observations prior to treatment and the first MTD observations obtained after treatment onset, i.e., the observations obtained in the first 3 months of treatment. If, for a given patient, no observations were available prior to treatment, we used only the MTD observations obtained within the first 3 months after treatment onset. Patients for whom no information was available for the first 3 months of treatment were excluded from the analysis. Overall, data from 45 patients were analyzed. Among these, 31 patients had a single MTD observation during the first 3 months of treatment, and 14 patients had two MTD observations. When possible, MTD observations before treatment onset were used to estimate empirical Bayes estimates (EBEs) of the disease-specific parameters of the model. The MTD observations after treatment start were then used to estimate the treatment-specific parameters of the model. EBEs were calculated using MatLab (MathWorks, Natick, MA) after the population parameters were estimated with Monolix.

To evaluate the capacity of the model to predict individual tumor response to TMZ treatment, two clinically relevant metrics were calculated: the duration of response, i.e., the length of time during which MTD decreases, and the minimal tumor size reached as a result of TMZ effect.

External analysis

In the analysis described above, the model's predictive capacity was assessed on patients whose full time-course

data were used to estimate the population parameters; these population parameters constituted prior information for the calculation of EBEs. To explore whether this caused a bias, we subsequently performed predictive analysis on the 43 "external" patients whose data had been excluded from the initial model-building process, owing to a lack of genetic information. In this case, we used early MTD observations as in the original predictive analysis, but without covariates.

We then used population parameters to simulate 200 new virtual patients, and we made predictions for these patients using the model without covariates in a first step, and we incorporated genetic statuses into the predictions in a second step.

RESULTS

Tumor size time-course in patients treated with temozolomide

Figure 1 depicts the time-course of tumor size (mean tumor diameter) in the 77 LGG patients included in the analysis. Patients received a median of 18 TMZ cycles (minimum 2 cycles, maximum 24). **Table 1** shows a summary of the characteristics of the 77 patients. Tumor size increased linearly before treatment.[22] After TMZ onset, an initial MTD decrease followed by a MTD reincrease was observed ($n = 58$, 75%). Median time to tumor progression was 18 months. In 34 patients MTD a reincrease occurred during TMZ treatment while in 24 patients it occurred after TMZ discontinuation. We separated the patients to present tumor profiles in a clear manner, but it did not impact data analysis.

Mathematical model of LGG response to temozolomide

Inclusion of a resistance term for the proliferative tissue resulted in a significantly better model fit (drop of 200 points in the objective function) compared with exclusion of the resistance term. The model with the inclusion of a resistance term for the quiescent tissue performed worse. However, because quiescent cells have the capacity to repair their DNA lesions, they also contribute to the emergence of resistance by repopulating the proliferative compartment. Thus, the final selected model incorporated a resistance term for the proliferative tissue only:

$$drug_{induced_{decay}} = \gamma \times KDE \times P \times C \times e^{-res.t} \tag{2}$$

The term *res* denotes the resistance parameter. Given the time scale of data collection compared to the time scale of TMZ delivery scheduling, we represented a single TMZ cycle (actually composed of five daily administrations) as a single bolus administration with corresponding concentration, *C*, assumed to undergo exponential decay at a constant rate *KDE* (a so-called K-PD approach[23]). The population value of *KDE* parameter was fixed to 8.3 $month^{-1}$ corresponding to a half-life of 2.5 days, allowing for a residual active concentration of TMZ after 5 days of treatment. The parameter γ is the constant rate for proliferative tissue death (also referred to as the TMZ efficacy parameter). A schematic view of the model is
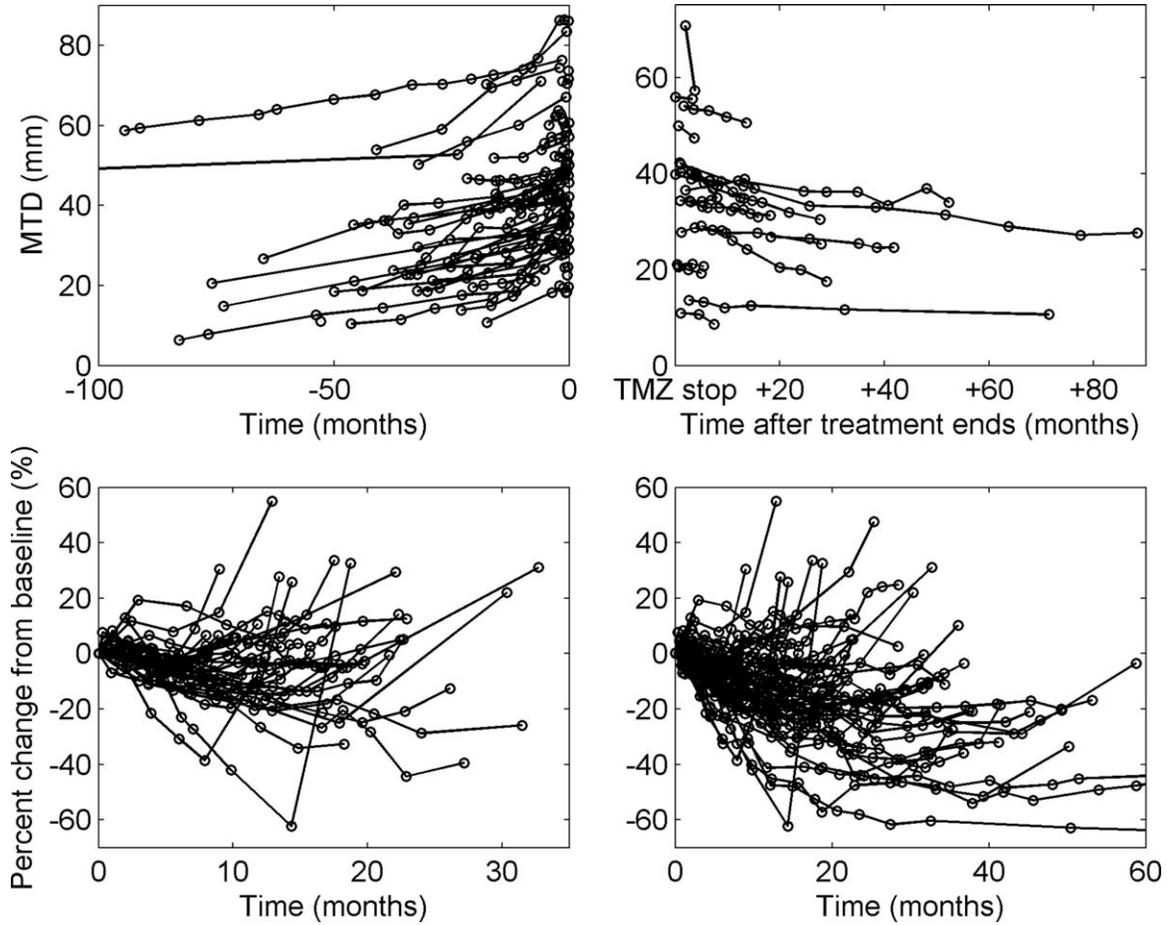
Figure 1 Typical tumor size dynamics for the 77 patients included in the analysis. Top, left: MTD time-course before treatment onset ($n = 77$). Top, right: In 21 patients, an ongoing MTD decrease after treatment discontinuation was observed. Bottom, left: Acquired resistance occurs in 34 patients. MTD time-course shows initial decrease followed by progression during TMZ treatment. Bottom, right: MTD time-course exhibits initial decrease followed by progression before or after treatment cessation ($n = 58$).

presented in **Figure 2**. The full mathematical equations of the model are:

$$\frac{dC}{dt} = -KDE \times C, \quad C(0) = 0$$

$$\frac{dP}{dt} = \lambda_P \times P\left(1 - \frac{P^*}{K}\right) + k_{Q_pP} \times Q_p - k_{PQ}$$
$$\times P - \gamma e^{-\text{res.}t} \times C \times KDE \times P, \quad P(0) = P_0$$

$$\frac{dQ}{dt} = k_{PQ} \times P - \gamma \times C \times KDE \times Q, \quad Q(0) = Q_0$$

$$\frac{dQ_p}{dt} = \gamma \times C \times KDE \times Q - k_{Q_pP}Q_p - \delta_{Q_p}Q_p, \quad Q_p(0) = 0$$

$$P^* = P + Q + Q_p$$

Overall, the model includes seven parameters and two initial conditions. Two parameters are disease-specific and related to tumor growth: the proliferation rate (λ_P) and the transfer constant rate (k_{PQ}) from proliferation to quiescence. The five remaining parameters are related to TMZ action

and effect and are called treatment-specific parameters. In particular, the constant rate of death of quiescent cells is denoted δ_{Q_p} and k_{Q_pP} is the constant rate of transition from quiescence to proliferation following repair of TMZ-induced DNA damage. For identifiability reasons, we assumed that the initial drug effect is the same on P and Q. This is consistent with the biology, as TMZ acts on cells regardless of their stage in the division process.

Impact of molecular status on tumor size dynamics
The covariate analysis performed with the three molecular status characteristics showed that p53 mutation could be included as a covariate of the TMZ efficacy parameter (γ). On the basis of the stepwise forward/backward analysis, we further determined that chromosomal 1p/19q codeletion could be included as a covariate on the constant rate k_{Q_pP} (transition from quiescence to proliferation following repair of TMZ-induced DNA damage. The inclusion of these two model covariates led to a significant drop in the objective function (126 points; $P < 0.01$, likelihood-ratio test). In the

Table 1 Main characteristics of the 77 low-grade glioma patients included in the internal analysis and 43 patients used for external validation

	Internal patients $N = 77$	External patients $N = 43$
Demographic		
Sex, M/F	42/35	25/18
Median age at treatment onset	40 (25–71)	48 (24–72)
Molecular status		
1p-19q co-deleted/1p-19q non-co-deleted	23/47	–
p53 mutated/p53 nonmutated	24/35	–
ID mutated/IDH nonmutated	35/19	–
Histological type		
Oligodendrogliomas	56	33
Oligoastrocytomas	16	6
Astrocytomas	5	4
Treatment		
Median number of TMZ cycles	18 (2–24)	18 (4–30)
Median interval between TMZ cycles	31 (21–45)	31 (24–50)
Tumor response		
Median time to progression (months)	14.5 (4–90)	12.8 (5–93)
Median duration of treatment (months)	18 (2–24)	18 (3–28)

stepwise analysis procedure, IDH mutation status identified as having an effect on model parameters when tested independently from the two other covariates was not identified as a significant covariate in the presence of p53 and 1p/19q information. This is in agreement with the known redundancy of the genetic information[24] and indicates that, in our model, p53 and 1p/19q information intrinsically integrate IDH information. The parameter estimates of the final model (including covariates) are presented in **Table 2**.

Among p53-mutated patients, the value of the TMZ efficacy parameter is 45% lower than among p53-nonmutated patients, suggesting that TMZ therapy is almost two times less effective in the former population. This is consistent with preclinical evidence that p53 mutations decrease sensitivity to TMZ in gliomas.[25,26] Likewise, among patients with the 1p/19q codeletion, the value of k_{Q_pP} is 15% lower than among non-codeleted patients, suggesting that among patients in the former group, DNA-damaged quiescent cells have less capacity to repair themselves. This finding is consistent with the longer duration of response reported in codeleted patients.[12]

Figure 3 shows goodness-of-fit (visual predictive check) plots for the 77 patients included in the model-building
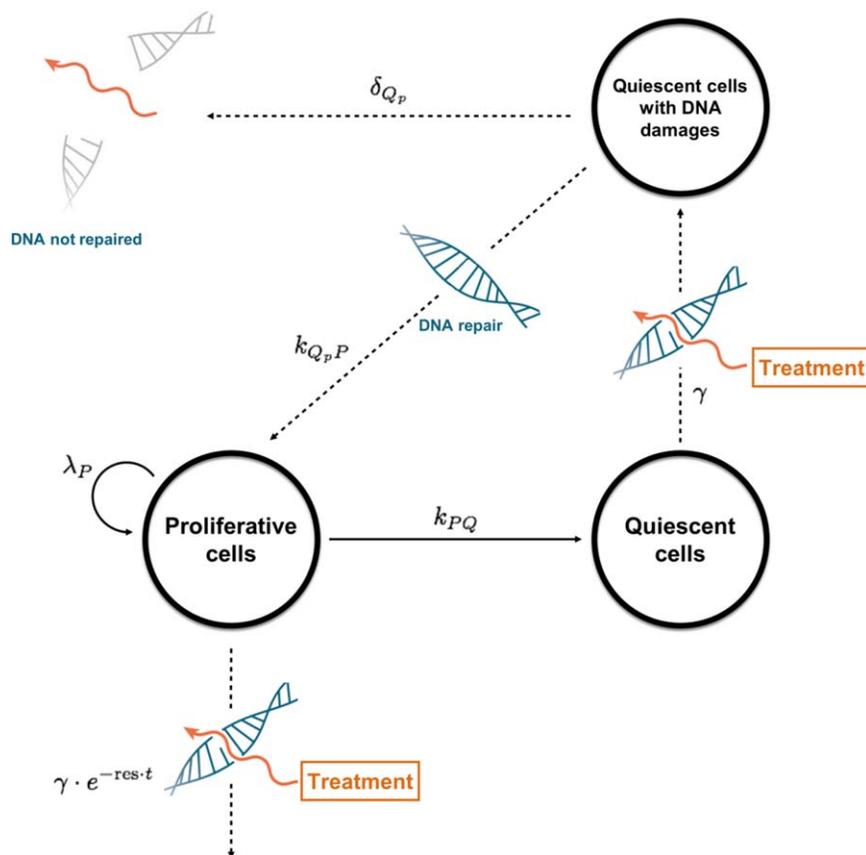

Figure 2 Schematic view of the model with model's parameters. *P* is the proliferative tissue, *Q* is the nondamaged quiescent tissue, and Q_p is the damaged quiescent tissue. The sum of the values corresponding to the three compartments, P^*, is compared to the MTD observations. Proliferative tissue (*P*) can become quiescent (*Q*). TMZ treatment affects both proliferative and quiescent tissues. Damaged quiescent tissue can either repair its DNA lesions and return to a proliferative state or die due to treatment-induced lesions.

Prediction of Low-Grade Glioma Response to TMZ
Mazzocco *et al*.

733

Table 2 Model parameter estimates with their standard deviations as well as covariate effects of 1p/19q codeletion and p53 mutations

Model parameters	Units	Estimates	CV (%)	η-shrinkage (%)
P_0	mm	1.72 (21)	143 (11)	18
Q_0	mm	32.1 (7)	55.8 (8)	2
λ_P	month^{-1}	0.143 (12)	63.1 (13)	23
k_{PQ}	month^{-1}	0.0429 (21)	81 (22)	47
k_{Q_pP} 1p19q non-codeleted	month^{-1}	0.00947 (42)	162 (16)	35
k_{Q_pP} 1p19q codeleted	month^{-1}	0.00807 (49)	–	–
δ_{Q_p}	month^{-1}	0.0188 (19)	86.2 (17)	32
γ p53 wild	–	0.254 (18)	68.6 (16)	34
γ p53 mutated	–	0.143 (19)	–	–
res	month^{-1}	0.1 (22)	80.5 (26)	57
KDE	month^{-1}	8.3 (FIXED)	50 (FIXED)	84
a	mm	1.73 (3)	–	–

Parameters are defined in the text. *a* is the parameter for the constant error model. The residual standard errors are shown in parentheses and are given as percentages of the estimate values. Interindividual variability (CV) is expressed as percentages. η-shrinkage,[37] indicating the tendency of individual parameters shrinkage towards population value is presented in the last column, and η-shrinkage[37] was evaluated at 19%. All parameters were estimated with relative standard errors less than 50%.

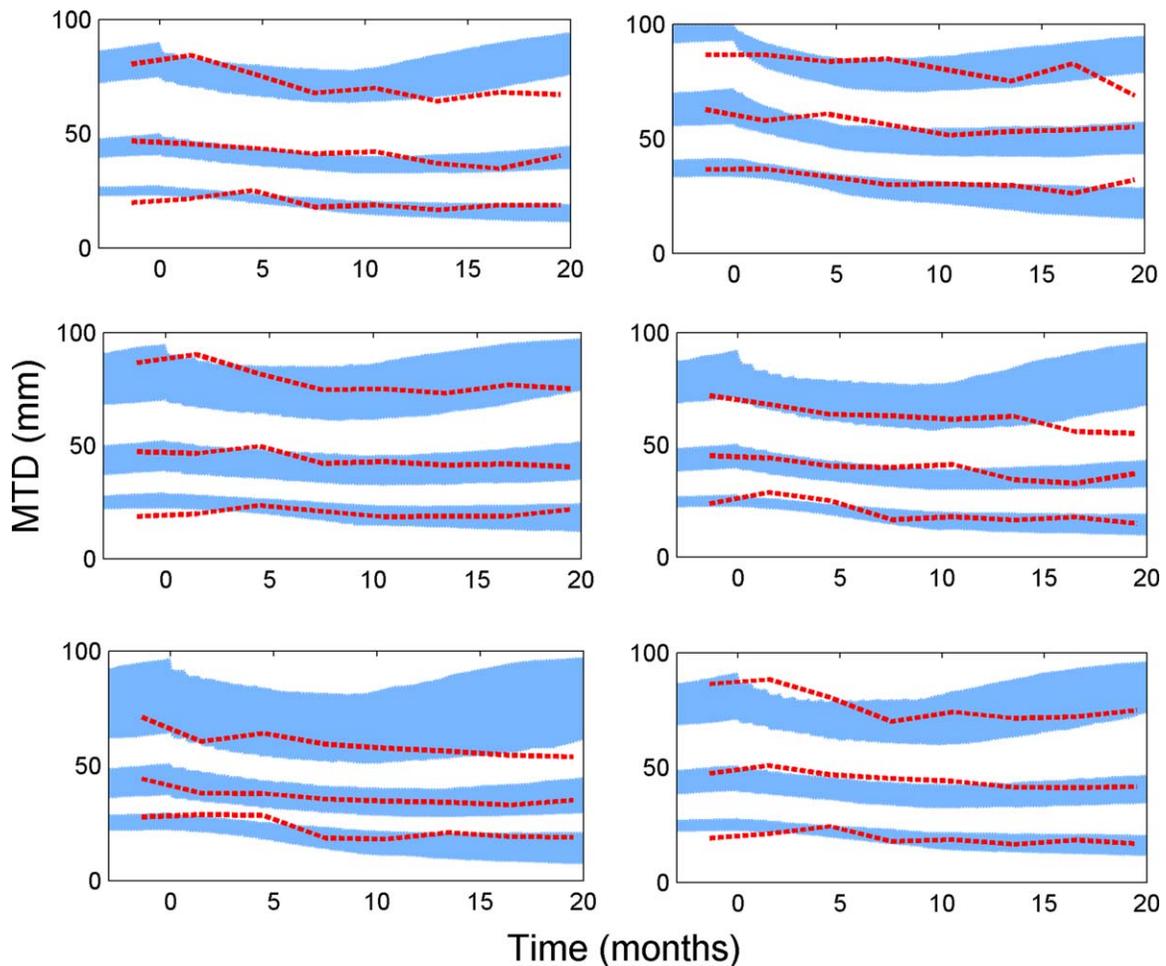**Figure 3** Top, Left: Visual Predictive Check (VPC) diagnostics on the 77 patients included in the (internal) analysis. Dashed lines represent the 5th, 50th, and 95th percentiles from observed data. The areas represent the 90% confidence interval of the 5th, 50th, and 95th simulated percentiles. Top, Right: VPC on 43 external patients. Middle, Left: VPC for the internal patients with p53 mutation (*n* = 24). Middle, Right: p53 nonmutated patients (*n* = 35). Bottom, Left: VPC for 1p/19q codeleted patients (*n* = 23). Bottom, Right: VPC for 1p/19q non-codeleted patient (*n* = 47).
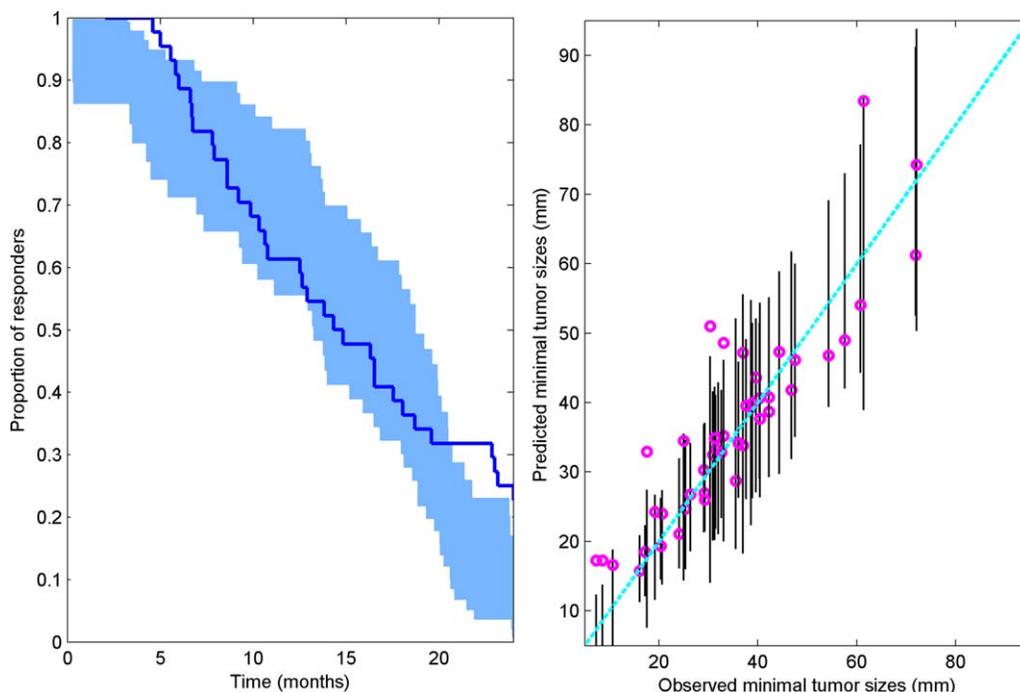
Figure 4 Left: Kaplan-Meier curve for observed times to tumor growth together with a model-based confidence interval. Right: Predicted minimal tumor sizes vs. observed minimal tumor sizes. The vertical lines represent a tolerance of 25% relative to tumor size at treatment onset. Both times to tumor growth and minimal tumor size were predicted using the observations up to the end of the 3rd month of treatment.

dataset and for the 43 patients included in an external dataset. These diagnostics indicate good quality of the model, with and without covariates. The proposed model is able to capture the variability in patients' response to TMZ, including prolonged response after therapy discontinuation or emergence of acquired resistance to TMZ during treatment.

Prediction of response to TMZ chemotherapy

Figure 4 shows predictions regarding individual patients' response durations (left-hand side), represented by Kaplan-Meier curves, together with observed response durations that fall in the 95% confidence interval (CI) for almost 2 years after treatment onset. Beyond 2 years, the model predictions are incorrect, which is not surprising given that only information until month 3 is taken into account. Notably, beyond 2 years predicted times to progression are earlier than the actual times to progression. In this respect, the modeling framework shows a tendency for underestimating the effect of the treatment. The early part of the Kaplan-Meier curve also indicates a tendency to predict progression at a very early time. For a small subset of patients ($n = 4$), the unique MTD point during the first 3 months of treatment was greater than the MTD at treatment onset, while successive MTD points showed a significant response. Integrating this point in our modeling framework resulted in predicting very early progression. However, removing these four patients resulted in correcting the early part of the Kaplan-Meier curve.

Figure 4 also shows predicted vs. observed minimal tumor size (right-hand side). We evaluated prediction bias

(mean prediction error) and precision (root mean squared prediction error).[27] Prediction bias was 1.89 mm (95% CI (–0.22, 3.99)) and precision was 7.18 mm (95% CI (4.52, 9.10)). For 90% of the patients ($n = 40$), the observed minimal tumor size was predicted correctly, with less than 25% relative error (relative to tumor size at treatment onset); this corresponds, approximately, to an error of about 1 cm in MTD. Notably, for each of the 14 patients with two MTD observations within the 3 first months of treatment, the minimal tumor size was predicted with an error of less than 15% (about 6 mm).

Individual predictions for six patients with repeated measurements during the first 3 months of treatment are displayed in **Figure 5** as an illustration of the method proposed herein. It shows that the model is also able to predict tumor time-course, especially for these patients. For the 10% of patients ($n = 5$) for whom predictions of minimal tumor size were incorrect, we observed that, for four of them, tumor size reduction was unexpectedly characterized by two phases: an initial moderate decrease in tumor size within the first 5 months of treatment, followed by a more pronounced decrease after 5 months. For these four patients, the model underevaluated the response. Inclusion of a second MTD observation (obtained after 5 months of treatment) yielded correct minimal tumor size predictions for these patients. Tumor response for one additional patient could not be predicted owing to his/her prolonged response to treatment (more than 40 months). The model may not be able to capture such extreme behavior.
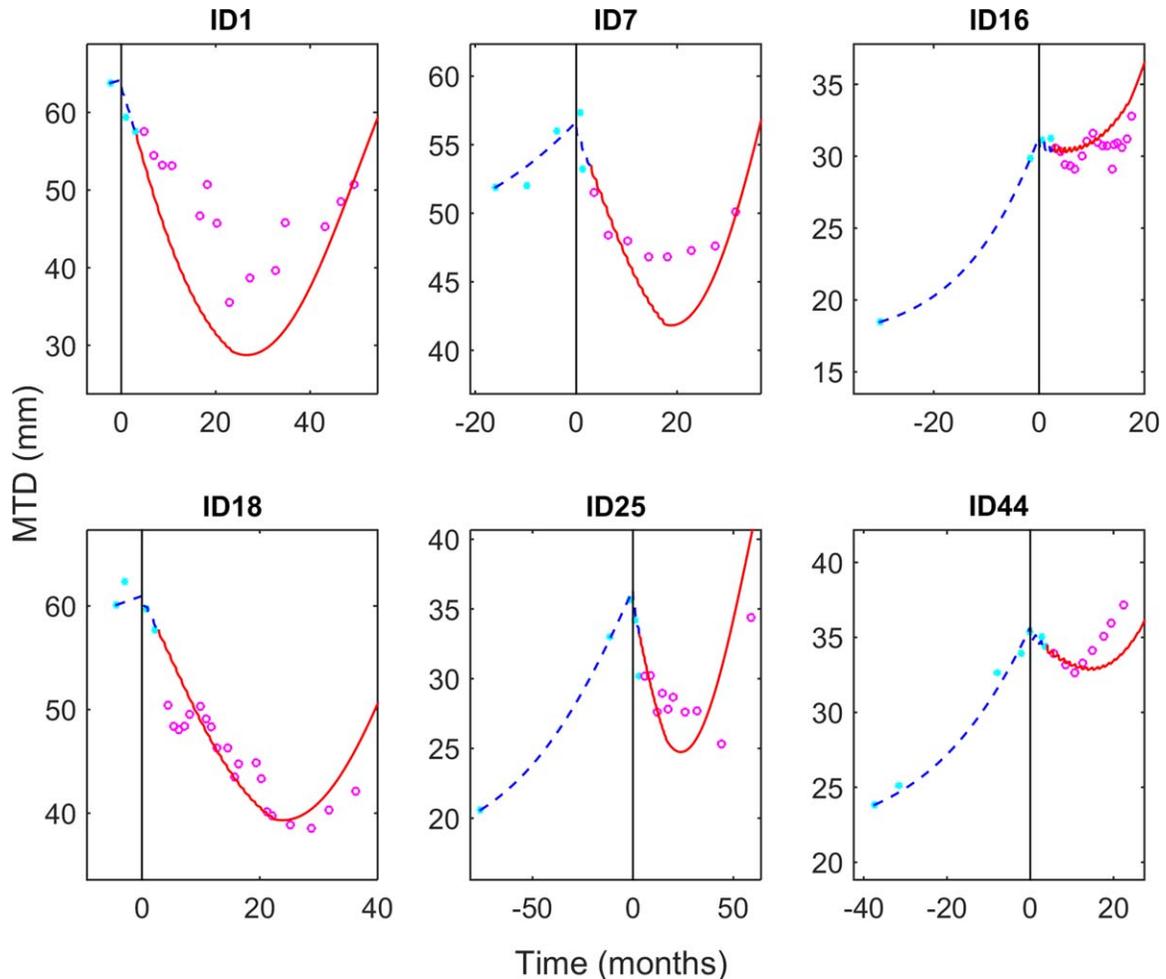
Prediction of Low-Grade Glioma Response to TMZ
Mazzocco *et al*.

735

Figure 5 Individual tumor size predictions for six patients with repeated assessment of tumor response during the first 3 months of treatment. Filled circles represent tumor sizes that are used to estimate individual parameters, and empty circles are observations to be predicted. The dashed lines represent tumor dynamics simulated until the 3rd month of treatment, and the solid line represents the actual prediction.

We then performed predictive analysis on the 43 "external" patients. The model successfully predicted the minimal tumor size for 75% of these patients (bias −4.41 mm (−7.14, −1.67)). To evaluate whether the reduction in predictive capability was due to the lack of genetic information or to the fact that these patients' data were not incorporated as prior information in model-building, we made predictions for 200 virtual patients. Without covariates, the minimal tumor size was successfully predicted for 76% of the virtual patients. When we incorporated genetic statuses, predictive capacity rose to 87% (bias 0.31 mm (−0.86, 1.49)). These observations lead us to believe that the reduction in the model's predictive capacity for the 43 external patients was mainly due to the absence of genetic information.

DISCUSSION

Molecular profiling of tumors is a well-known strategy to personalize anticancer treatments. Another approach is

mathematical modeling.[28,29] Mathematical models of tumor growth and response to treatment allow characterizing quantitatively the efficacy and toxicity of anticancer agents and can be used to predict clinical response.[7,30] In the present study, we show that combining longitudinal tumor size measurements through the use of quantitative modeling with a tumor's genetic characterization is a promising strategy to personalize treatments in patients with low-grade gliomas.

Using p53 mutation and 1p/19q codeletion as covariates significantly improved the model accuracy. In agreement with the literature, p53 and 1p/19q molecular statuses significantly impacted the dynamics of LGG response to treatment: p53 mutation impaired TMZ efficacy and 1p/19q codeleted tumors had less ability to repair TMZ-induced DNA lesions in quiescent tissue, thus increasing the overall efficacy of treatment. IDH mutation status did not provide useful information on tumor size dynamics beyond the combined information provided by p53 and 1p/19q status. However, it would be relevant to introduce IDH status as a

Prediction of Low-Grade Glioma Response to TMZ
Mazzocco *et al*.

736

model covariate in cases in which p53 and 1p/19q information is not available for a given patient.

Molecular information (p53 and 1p/19q status) and tumor observations obtained during the first 3 months after TMZ treatment onset were sufficient to correctly predict the amplitude of response and its duration for almost 2 years, especially in those patients in whom precise assessment of early tumor response was available. An adaptive approach, consisting of updating the model predictions at each new MTD observation, could be implemented to prolong the validity period of the prediction and to enhance the percentage of patients for whom the minimal tumor size is successfully predicted. These results, however, need to be confirmed in a larger set of external patients. It would also be interesting to evaluate the relationship between the predictive performance of the model and the timing of MTD observations used for predictive purposes. In this study, we focused on MTD observations obtained during the first 3 months of treatment because we wanted to obtain a reference or rational value for the predictive potential of the model. In the area of brain tumor, numerous studies have used partial differential equation models integrating both time dynamics and spatial aspects of these highly diffusive malignancies (see refs. 31,32 for examples). It would also be important to apply the same prediction framework with these types of models, which capture more precisely glioma evolution.

Emergence of acquired resistance, defined as progression after initial benefits, is a critical issue in clinical oncology and model-based approaches should be used to better understand, characterize, and predict this phenomenon. Mechanisms of acquired resistance can be pharmacological resulting from decreased drug uptake into the cell, intracellular drug inactivation, or repair of drug-induced damages. This is the case of the LGG response to TMZ, for which it has been shown that more than 90% of recurrent gliomas show no response to a second treatment with TMZ.[33] One of the key elements in TMZ resistance is MGMT, an enzymatic protein with the faculty to repair the principal O^6-meG-alkylation site to TMZ,[34] thus resulting in decreased efficacy of drugs during treatment. MGMT could not be tested as a covariate in our model since for most patients only formalin-fixed paraffin-embedded (FFPE) tissue was available for DNA tests, whereas MGMT methylation testing ideally needs frozen tissue. Of note, resistance to TMZ is also responsible for significant therapeutic failures in melanoma.[35] Following this biological knowledge, we modeled acquisition of resistance by decreasing drug efficacy on LGG proliferative tissue with time following therapy onset. Since all patients received the same TMZ doses with the same scheduling, we believe that modeling resistance as a function of actual drug exposure would not have led to significantly different results. For identifiability reasons, we could not model all transitions between the three compartments, especially the possibility for quiescent cells to directly return into proliferation, as it could occur without treatment. However, during treatment quiescent cells do have the capacity to repair their DNA and become proliferative. Therefore, this model is a relevant tool to characterize

tumor response to TMZ but does not aim to faithfully mimic natural tumor growth. Our model is flexible enough to reproduce the variability of patients' response to standard TMZ protocol and has the capacity to mimic both tumor regrowth during treatment as a result of acquired resistance to TMZ and prolonged response to treatment.

Finally, our model could constitute a rational tool to optimize the duration of temozolomide therapy in low-grade glioma patients. Up to now, there are no clear rules or guidelines regarding the optimal number of cycles or treatment duration in patients treated with TMZ.[15] Many neuro-oncologists prolong the duration of the treatment beyond 12 cycles if an ongoing decrease in tumor size is observed at this time. However, there are downsides to prolonging TMZ treatment, including side effects and costs. An even greater concern is that TMZ therapy might drive the evolutionary path to high-grade glioma.[36] Consequently, determining the optimal duration of TMZ therapy and maximizing the duration of the response is a critical challenge in the management of LGG. Using our model as a simulation tool to determine the optimal number of TMZ cycles each patient should have received, we found that for 47% of the 45 patients analyzed ($n = 21$), the model would have recommended, by month 3 after treatment onset, administration of additional TMZ cycles beyond what these patients actually received; i.e., in these patients delivery of additional TMZ could have resulted in tumor shrinkage exceeding what was ultimately achieved. In contrast, the model predicted that 33% of the patients ($n = 15$) could have benefited if their treatment had been stopped earlier than it actually was.

Mandonnet *et al*. suggested that knowledge of the glioma growth rate prior to treatment can be used to optimize patient management and follow-up.[22] Our approach proposes to leverage early tumor dynamical information together with the a tumor's genetic characteristics to predict tumor size response. We believe that this framework can be used as a template for other diseases whose response to treatment is characterized by emergence of acquired resistance.

Conflict of Interest. No conflicts of interest to declare.

1. Eisenhauer, E. *et al.* New response evaluation criteria in solid tumours: revised RECIST guideline (version 1.1). *Eur. J. Cancer* **45**, 228–247 (2009).
2. Van den Bent, M.J. *et al.* Response assessment in neuro-oncology (a report of the RANO group): assessment of outcome in trials of diffuse low-grade gliomas. *Lancet Oncol.* **12**, 583–593 (2011).
3. Ratain, M.J. & Eckhardt, S.G. Phase II studies of modern drugs directed against new targets: if you are fazed, too, then resist RECIST. *J. Clin. Oncol.* **22**, 4442–4445 (2004).

Prediction of Low-Grade Glioma Response to TMZ
Mazzocco *et al*.

737

4. Sharma, M.R., Maitland, M.L. & Ratain, M.J. RECIST: no longer the sharpest tool in the oncology clinical trials toolbox—point. *Cancer Res.* **72**, 5145–5149; discussion 5150 (2012).

5. Wang, Y. *et al.* Elucidation of relationship between tumor size and survival in non-small-cell lung cancer patients can aid early decision making in clinical drug development. *Clin. Pharmacol. Ther.* **86**, 167–174 (2009).

6. Ribba, B. *et al.* A review of mixed-effects models of tumor growth and effects of anti-cancer drug treatment for population analysis. *CPT Pharmacometrics Syst. Pharmacol.* **3**, e113 (2014).

7. Bender, B.C., Schindler, E. & Friberg, L.E. Population pharmacokinetic pharmacodynamic modelling in oncology: a tool for predicting clinical response. *Br. J. Clin. Pharmacol.* 1–42 (2013).

8. Bruno, R., Mercier, F. & Claret, L. Evaluation of tumor size response metrics to predict survival in oncology clinical trials. *Clin. Pharmacol. Ther.* **95**, 386–393 (2014).

9. Claret, L. *et al.* Model-based prediction of phase III overall survival in colorectal cancer on the basis of phase II tumor dynamics. *J. Clin. Oncol.* **27**, 4103–4108 (2009).

10. Soffietti, R. *et al.* Guidelines on management of low-grade gliomas: report of an EFNS-EANO Task Force. *Eur. J. Neurol.* **17**, 1124–1133 (2010).

11. Kujas, M. *et al.* Chromosome 1p loss: a favorable prognostic factor in low-grade gliomas. *Ann. Neurol.* **58**, 322–326 (2005).

12. Ricard, D. *et al.* Dynamic history of low-grade gliomas before and after temozolomide treatment. *Ann. Neurol.* **61**, 484–490 (2007).

13. Houillier, C. *et al.* IDH1 or IDH2 mutations predict longer survival and response to temozolomide in low-grade gliomas. *J. Clin. Oncol.* **22**, 3133–3138 (2004).

14. Hoang-Xuan, K. *et al.* Temozolomide as initial treatment for adults with low-grade oligodendrogliomas or oligoastrocytomas and correlation with chromosome 1p deletions. *J. Clin. Oncol.* **22**, 3133–3138 (2004).

15. Weller, M. Chemotherapy for low-grade gliomas: when? how? how long? *Neurol. Oncol.* **12**, 1013 (2010).

16. Ribba, B. *et al.* A tumor growth inhibition model for low-grade glioma treated with chemotherapy or radiotherapy. *Clin. Cancer Res.* **18**, 5071–5080 (2012).

17. Gillet, E. *et al.* TP53 and p53 statuses and their clinical impact in diffuse low grade gliomas. *J. Neurooncol.* 131–139 (2014).

18. Kaina, B. DNA damage-triggered apoptosis: critical role of DNA repair, double-strand breaks, cell proliferation and signaling. *Biochem. Pharmacol.* **66**, 1547–1554 (2003).

19. Masunaga, S. *et al.* Potentially lethal damage repair by total and quiescent tumor cells following various DNA-damaging treatments. *Radiat. Med.* **17**, 259–264 (1999).

20. Lindstrom, M. & Bates, D. Nonlinear mixed effects models for repeated measures data. *Biometrics* **46**, 673–687 (1990).

21. Wählby, U., Jonsson, E.N. & Karlsson, M.O. Comparison of stepwise covariate model building strategies in population pharmacokinetic-pharmacodynamic analysis. *AAPS PharmSci.* **4**, E27 (2002).

22. Mandonnet, E. *et al.* Continuous growth of mean tumor diameter in a subset of grade II gliomas. *Ann. Neurol.* **53**, 524–528 (2003).

23. Jacqmin, P. *et al.* Modelling response time profiles in the absence of drug concentrations: definition and performance evaluation of the K-PD model. *J. Pharmacokinet. Pharmacodyn.* **34**, 57–85 (2007).

24. Labussiere, M. *et al.* All the 1p19q codeleted gliomas are mutated on IDH1 or IDH2. *Neurology* **74**, 1886–1890 (2010).

25. Roos, W.P. *et al.* Apoptosis in malignant glioma cells triggered by the temozolomide-induced DNA lesion O6-methylguanine. *Oncogene* **26**, 186–197 (2007).

26. Hermisson, M. *et al.* O6-methylguanine DNA methyltransferase and p53 status predict temozolomide sensitivity in human malignant glioma cells. *J. Neurochem.* **96**, 766–776 (2006).

27. Sheiner, L.B. & Beal, S.L. Some suggestions for measuring predictive performance. *J. Pharmacokinet. Biopharm.* **9**, 503–512 (1981).

28. Wilbaux, M. *et al.* Prediction of tumour response induced by chemotherapy using modelling of CA-125 kinetics in recurrent ovarian cancer patients. *Br. J. Cancer* **110**, 1517–1524 (2014).

29. Wallin, J.E., Friberg, L.E. & Karlsson, M.O. A tool for neutrophil guided dose adaptation in chemotherapy. *Comput. Methods Programs Biomed.* **93**, 283–291 (2009).

30. Claret, L. *et al.* Evaluation of tumor-size response metrics to predict overall survival in Western and Chinese patients with first-line metastatic colorectal cancer. *J. Clin. Oncol.* **31**, 2110–2114 (2013).

31. Konukoglu, E. *et al.* Image guided personalization of reaction-diffution type tumor growth models using modified anisotropic eikonal equations. *IEEE Trans. Med. Imaging* **29**, 77–95 (2010).

32. Swanson, K.R., Alvord, E.C. Jr. & Murray, J.D. Virtual brain tumours (gliomas) enhance the reality of medical imaging and highlight inadequacies of current therapy. *Br. J. Cancer* **86**, 14–18 (2002).

33. Oliva, C.R. *et al.* Acquisition of temozolomide chemoresistance in gliomas leads to remodeling of mitochondrial electron transport chain. *J. Biol. Chem.* **285**, 39759–39767 (2010).

34. Kitange, G.J. *et al.* Induction of MGMT expression is associated with temozolomide resistance in glioblastoma xenografts. *Neurol Oncol.* **11**, 281–291 (2009).

35. Tentori, L., Lacal, P.M. & Graziani, G. Challenging resistance mechanisms to therapies for metastatic melanoma. *Trends Pharmacol. Sci.* **34**, 656–666 (2013).

36. Johnson, B.E. *et al.* Mutational analysis reveals the origin and therapy-driven evolution of recurrent glioma. *Science* **343**, 189–193 (2014).

37. Karlsson, M.O. & Savic, R.M. Diagnosing model diagnostics. *Clin. Pharmacol. Ther.* **82**, 17–20 (2007).

Supplementary information accompanies this paper on the *CPT: Pharmacometrics & Systems Pharmacology* website (http://www.wileyonlinelibrary.com/psp4)